Formation of PbSe Nanocrystals: A Growth toward Nanocubes

Weigang Lu and Jiye Fang*
Department of Chemistry and Advanced Materials Research Institute, University of New Orleans, New Orleans, Louisiana 70148

Yong Ding and Zhong Lin Wang*
School of Materials Science and Engineering, Georgia Institute of Technology, Atlanta, Georgia 30332-0245

Received: May 16, 2005; In Final Form: August 2, 2005

In this paper we report an electron microscopic observation of crystal shape development when PbSe nanocrystals were synthesized using a dynamic injection technique at different temperatures in the presence of oleic acid. A two-step evolution mechanism was proposed, indicating that the shape evolution of PbSe nanocrystals is dependent on the growth time, whereas the crystalline size can be tuned by varying the growth temperature under the studied conditions. It also implies that a higher growth rate in the ⟨111⟩ direction compared to that in the ⟨100⟩ direction results in the formation of nanocubes.

Lead chalcogenides are inspiring semiconductors with a narrow band gap. Size- and shape-controlled nanocrystals (NCs) of this family have demonstrated unique properties[1−5] and can potentially be employed in numerous applications, such as near-IR luminescence[6] and thermoelectric devices.[7,8] To produce monodisperse NCs of lead chalcogenides with high quality and tunable size and shape, it is significant to understand their NC formation process. Since the growth of PbS[9,10] and PbTe NCs[11] has been investigated previously, similar exploration on PbSe NCs should be conducted. Although the relationship between band gap and PbSe NC shape has been studied by Pietryga et al.[5] and the development of PbSe nanowires and nanorings has been achieved by Cho et al.[1] as well, efforts on observation of crystal shape development and understanding the possible mechanism of PbSe crystal evolution growth are still essential. In this paper, we concentrate on the time-dependent formation study of PbSe NCs based on our electron microscopic observation when a dynamic injection technique is applied to the synthesis.

PbSe NCs were prepared by rapidly injecting a phenyl ether solution of lead acetate and trioctylphosphine selenide ((TOP)-Se) into a vigorously stirred hot phenyl ether at 180 or 230 °C, in the presence of oleic acid.[12] In a typical experiment, Pb-$(Ac)_2$·$3H_2O$ (2.85 mmol), phenyl ether (15 mL), and oleic acid (3.0 mL) were mixed and heated to 150 °C for 30 min under an argon stream in a three-neck flask equipped with a condenser. After the solution was cooled to 40 °C, it was mixed with 4.0 mL of pre-prepared (TOP)Se solution (1 M for Se) in a glovebox. This mixture (10 mL) as a stock reactant was then rapidly injected into 15 mL of phenyl ether that was preheated to a certain temperature (180 or 230 °C) for 5 min with agitation in a similar device. In both cases, the temperature of the reaction system was lowered by ∼20−25 °C and then rapidly reached the desired value. A portion of the hot reaction mixture (2.0 mL) was extracted from the flask after a certain time of growth, and an equal volume of the premixed stock reactants was subsequently added into the flask under the argon stream. These operations of dynamic injections were successively conducted at an interval of every 5 min at a constant temperature. Each product was retrieved from the original solvent by centrifugation with an equal volume of ethanol as a polar solvent, redispersion in toluene, and evaluation under transmission electron microscopy (TEM) observation. Products were identified by TEM (JEOL 2010 TEM and Hitachi 2000 FE-TEM (FE = field emission) instruments) and by field emission scanning electron microscopy (SEM) (LEO 1530 FE-SEM instrument, operated at 5 and 10 keV). The phase of the nanocrystals was determined using an X-ray diffractometer (Philips X'pert system).

Upon injection, small PbSe clusters immediately nucleated and started to grow with stabilization provided by the capping ligands (TOP and oleic acid). We monitored the crystalline growth process by collecting small portions of the reacting solution from time to time for electron microscopic analyses. According to the general growth mechanism proposed in the La Mer model,[13] many systems exhibit an Ostwald ripening process. As a result, small clusters tend to grow into larger NCs to lower their surface energy.[14−16] Figure 1A,C demonstrates the images of 5-s-growth clusters based on bright-field and dark-field TEM determinations, respectively, revealing that small PbSe NCs (∼3−5 nm in size) tend to aggregate in the shape of an octahedron at a reaction temperature of 230 °C. The TEM diffraction pattern (Figure 1B) also indicates that these small NCs possess a cubic bulk rock-salt crystal structure with high crystallinity. The high-resolution TEM (HR-TEM) image further implies that most of the agglomerated particles have been coupled with each other (Figure 2), showing that the lattice planes of the depicted particles were mostly aligned. Moreover, it can be recognized that the lattice planes go straight through the contact areas, where the particles were epitaxially fused together, which is the foundation for agglomerating into a single larger size crystal.[17,18] On the basis of Murray's report,[8] PbSe NCs are quite easy to nucleate and grow even at a temperature of lower than 100 °C. The higher reaction temperature we applied would accelerate the chemical reaction and produce a burst of nucleation, which arouses the octahedral agglomerates.

According to our TEM observation presented in Figure 3A,B, most of the agglomerates can be developed into discrete

* To whom correspondence should be addressed. E-mail: jfang1@uno.edu (J.F.); zhong.wang@mse.gatech.edu (Z.L.W.).

10.1021/jp052573+ CCC: $30.25
Published on Web 09/21/2005

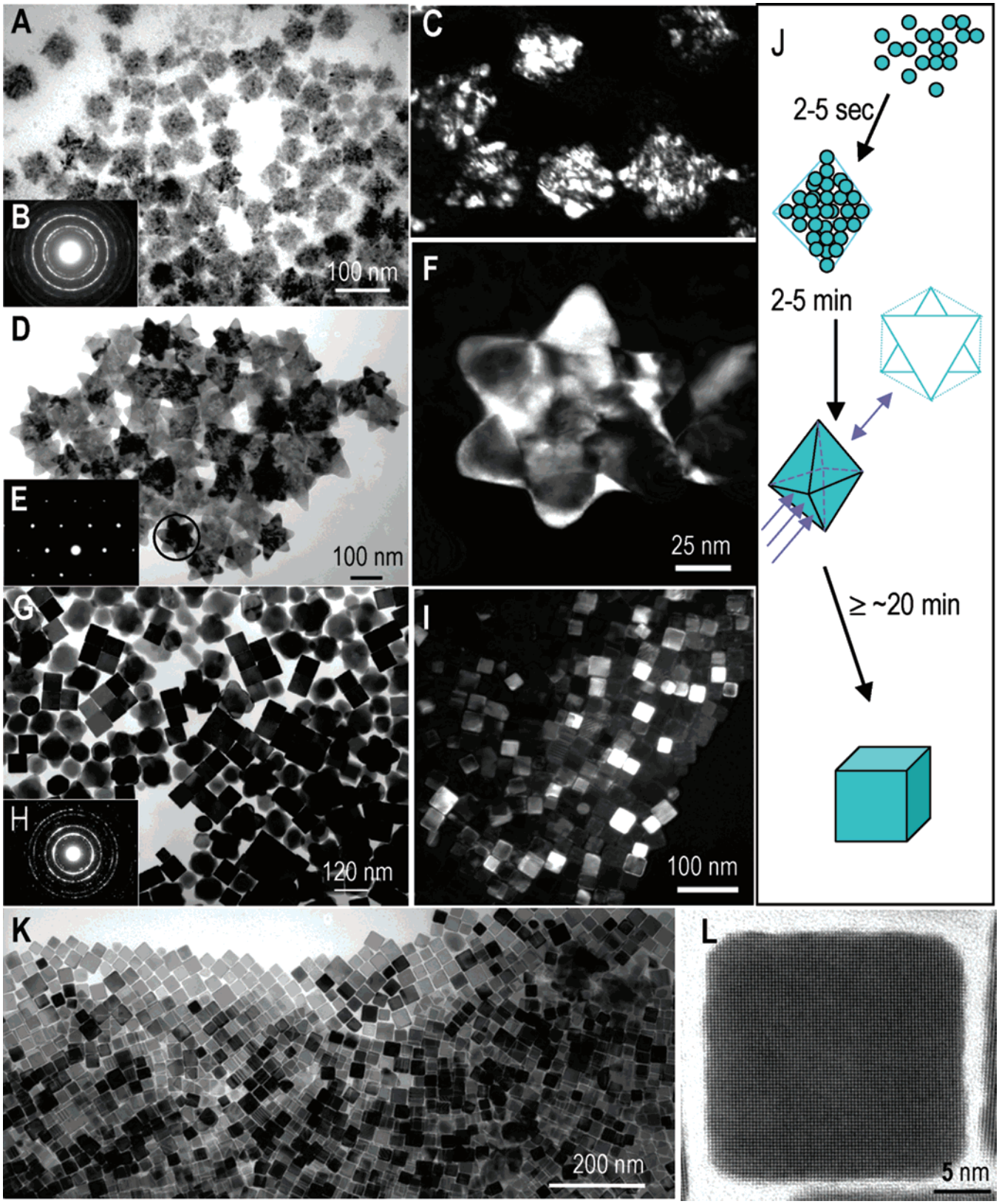

Figure 1. (A, C, B) TEM images and diffraction pattern of 5-s-growth PbSe clusters at 230 °C. (D, F, E) TEM images and diffraction pattern of a selected single PbSe octahedron grown for 2−5 min at 230 °C. (G, H) TEM image and diffraction pattern of PbSe nanocubes after five injections within a total aging time of ∼25 min at a growth temperature of 230 °C; (I, K, L) TEM images of a size-selected PbSe nanocube assembly and HR-TEM image of a single PbSe nanocube (the sample was grown through the same procedure at 180 °C for ∼25 min). (J) A scheme illustrating the formation process of PbSe nanocubes; (A), (D), (G), (K), and (L) are bright-field images, whereas (C), (F), and (I) are dark-field images.

hexagonal crystalline stars when the reaction time elapses for 20 s at 230 °C, although transitive morphology can still be detected. It is noted that the image corner of a single crystalline star (2D projection) is sharper than that containing small crystal agglomeration. As shown in Figure 1D, extension of the growth time to ∼2−5 min at 230 °C results in a further development

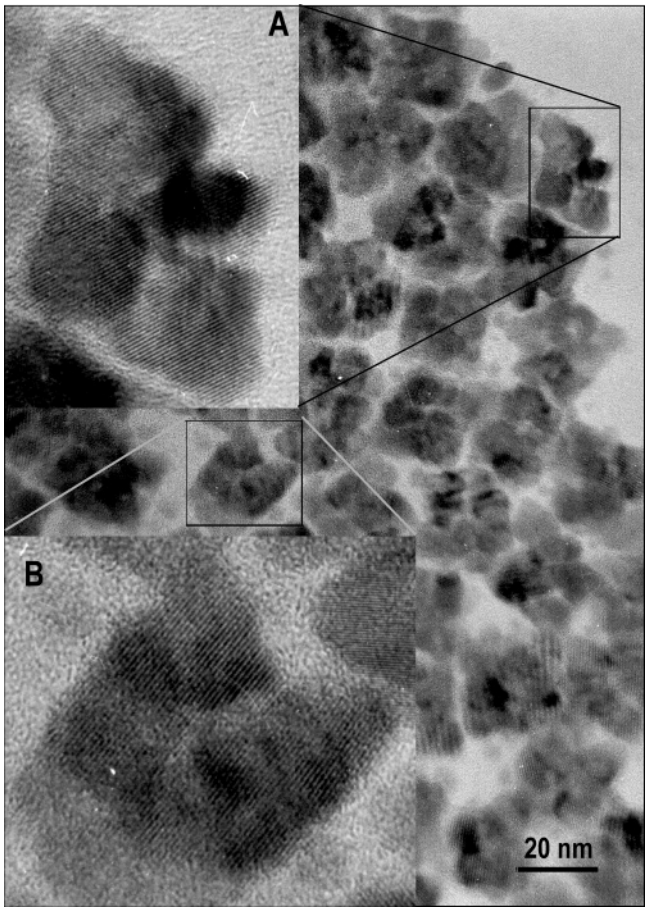

Figure 2. High-resolution TEM image, showing lattice planes of small particles restricted in the agglomerates. The sample was grown at 230 °C for 5 s.

of these PbSe stars, with a ~100 ± 10 nm diagonal. We realize that this profile star image was actually recorded from a projected shape of an octahedral crystal if viewing along [111] (see Figure 1J).[9,19] A dark-field TEM image (2D projection) of a single perfect PbSe star clearly exhibits the structural information of an octahedral NC along the [111] direction (Figure 1F). The electron diffraction pattern (Figure 1E) recorded on this selected NC verifies the zone axis of [111] and displays that the whole NC is a single crystal. The XRD trace of the PbSe octahedrons is presented in Figure 4 as well, in which all of the detectable peaks are indexed to almost the same positions as those from a standard bulk of PbSe (JCPDS-ICDD card 06-0354). In addition, the observation of the octahedral PbSe NCs was further supported by a collection of dark-field TEM images of the NC prepared at 180 °C at different tilt angles as indicated in Figure 3C,D. The 3D shape and the six projected corners of the octahedron are clearly presented by the dark-field images in Figure 3C,D, which also indicate the single-crystal nature of each octahedron. The HR-TEM image recorded from a corner of an octahedron apparently shows its high crystallinity and sharp surfaces (Figure 3E). Furthermore, the low-magnification SEM image (Figure 5A) also implies that PbSe octahedrons, as intermediate NCs produced at 180 °C, are uniform and high in yield.

To further develop the NCs into nanocubes, it is necessary to successively introduce additional reaction precursors for compensating the consumption of feedstock by the growing colloidal octahedrons[16] and to make the system more "open". In this work, we conducted a dynamic injection technique that was employed previously.[12,20] The advantage of this dynamic

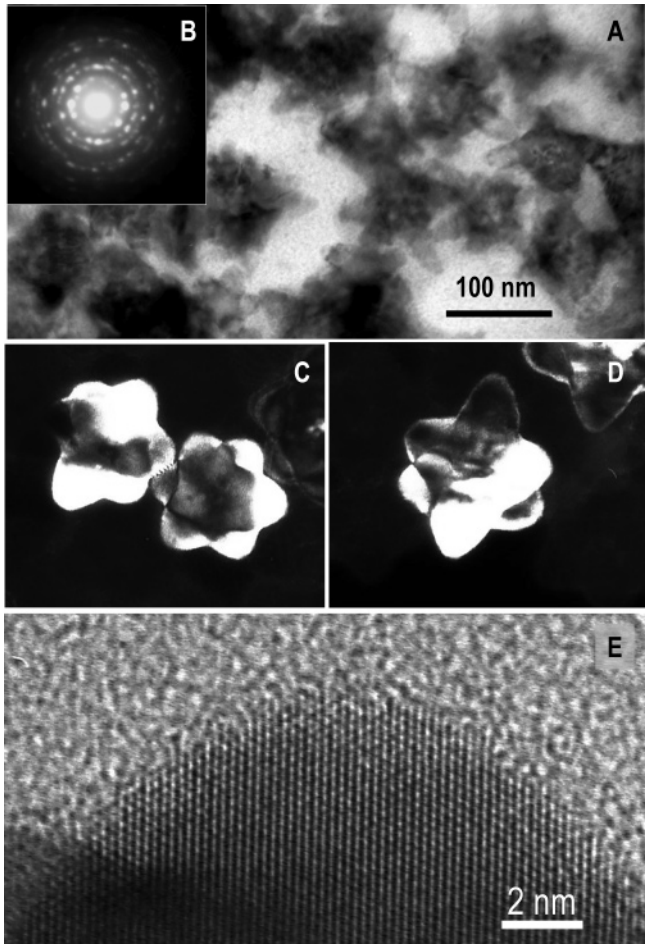

Figure 3. (A) TEM image of PbSe aggregates being grown at 230 °C for 20 s. (B) Diffraction pattern of the sample grown at 230 °C for 20 s. (C, D) Dark-field TEM images of single octahedral PbSe NCs at different tilt angles. (E) High-resolution TEM image recorded from a corner of such an octahedron. From (C) to (E), the sample was processed at 180 °C for 2 min.

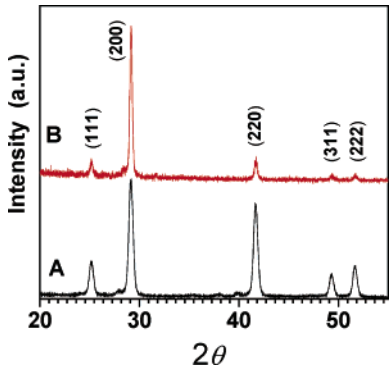

Figure 4. XRD traces of self-assembled PbSe NCs on a Si surface: (A) octahedrons; (B) nanocubes. Both samples were processed at 230 °C.

multi-injection is that primary precursors can be replenished so that enough primary PbSe clusters are provided to keep a constant rate of the crystal growth. As a result, cubic NCs as the major component could be detected in the final production after five injections within a total aging time of ~25 min at a growth temperature of 230 °C. Figure 1G is a bright-field TEM image of these NCs, indicating that a cubic shape dominates the morphology of the as-produced NCs. The pattern of electron diffraction (Figure 1H) from restricted nanocubes on a TEM grid exhibits high crystallinity. Similar to the discussion of PbTe

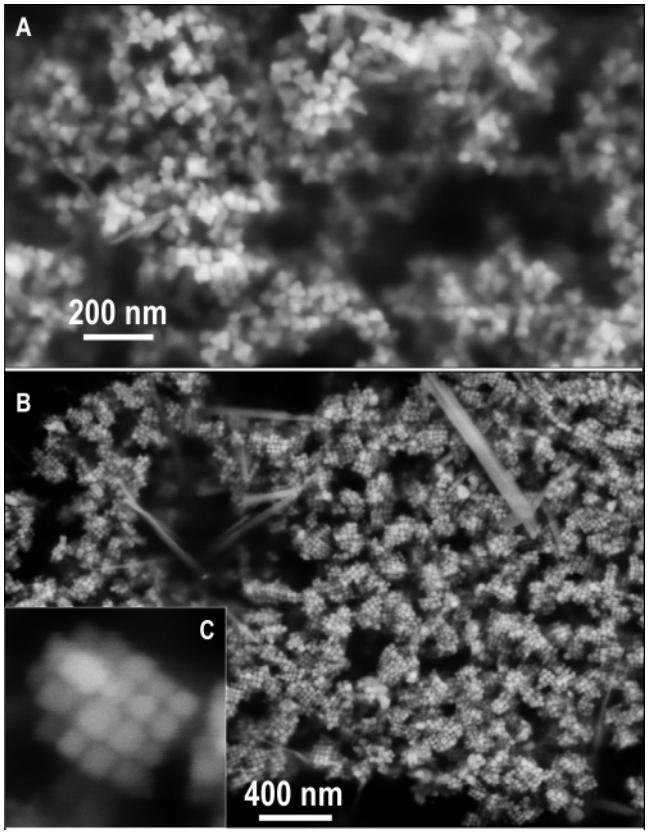

Figure 5. (A) SEM image of uniform PbSe NCs produced at 180 °C, confirming the existence of octahedrons as transitive intermediates. (B) SEM image of PbSe nanocubes synthesized at 180 °C (the sample was observed before size-selection treatment).

NC shape evolution,[11] the crystal morphology of PbSe NCs is dependent on the growth ratio between the ⟨100⟩ and ⟨111⟩ directions. The driving force of the evolution from octahedrons (which are presented as stars in a TEM image) to cubes may lie in the fact that the growth rate in the ⟨111⟩ direction is higher than that in the ⟨100⟩ direction,[18] although this type of growth results from various competitive factors such as crystalline size, growth temperature, the energy contributions from different parts of a crystal (such as the interfaces, edges, and corners), and the kinetics.[9,21] Cheon et al. once studied the evolution of PbS NCs, concluding a similar insight into growing PbS nanocubes as well.[9] In comparison with this observation, we have also successfully prepared PbSe nanocubes at a low growth temperature, 180 °C, using the same procedure of dynamic injection and growth time. SEM images of the nanocubes before size-selection treatment are presented in Figure 5B,C, revealing that the cubic NCs softly aggregated group-by-group for possibly minimizing their surface energy. The bright-field and dark-field TEM images of a size-selected PbSe nanocube assembly, presented in parts K and I of Figure 1, respectively, demonstrate perfect orientation order in 2D self-assembly. The HR-TEM image (Figure 1L) illustrates the cubic lattice structure and its high crystallinity as well. These observations indicate that a decrease of the growth temperature from 230 to 180 °C results in a reduction of the crystalline size by as much as half. However, a cube is still the dominant shape of these nanocrystals as long as the total aging time is ∼25 min. We further examined this sample grown at 180 °C using a powder XRD diffraction technique, demonstrating that the intensity of diffraction peak (200) was relatively enhanced very much (Figure 4B). This observation implies the presence of nanocubes perfectly assembled on the surface of the Si substrate,[11,22] because only the (200) facets have a chance to be diffracted in this case.

In summary, we have monitored the crystal shape development of PbSe NCs in high-temperature organic solution by using a growth technique of dynamic injection, and determined a two-step evolution mechanism: from nucleation to a single-crystalline octahedron (nanostar) and from a hexagonal nanostar to a nanocube. Basically, the shape evolution of PbSe NCs is dependent on the growth time, whereas the crystalline size can be tuned by varying the growth temperature under the described conditions. We also realize that the higher growth rate in the ⟨111⟩ direction compared to that in the ⟨100⟩ direction results in the formation of nanocubes. Understanding the crystallographic shape evolution and predicting the final architectures of lead chalcogenide NCs would favor the controlled synthesis of nano building blocks as well as the investigation of relevant unique properties of these NCs.

Acknowledgment. This work was supported by the NSF CAREER program (Grant DMR-0449580), NSF NIRT program (Grant ECS-0210332), DARPA program (Grant HR011-05-1-0031), and BSST LLC.

References and Notes

(1) Cho, K.-S.; Talapin, D. V.; Gaschler, W.; Murray, C. B. *J. Am. Chem. Soc.* **2005**, *127*, 7140−7147.
(2) Sirota, M.; Minkin, E.; Lifshitz, E.; Hensel, V.; Lahav, M. *J. Phys. Chem. B* **2001**, *105*, 6792−6797.
(3) McDonald, S. A.; Konstantatos, G.; Zhang, S.; Cyr, P. W.; Klem, E. J. D.; Levina, L.; Sargent, E. H. *Nat. Mater.* **2005**, *4*, 138−142.
(4) Allan, G.; Delerue, C. *Phys. Rev. B: Condens. Matter Mater. Phys.* **2004**, *70*, 245321/1−9.
(5) Pietryga, J. M.; Schaller, R. D.; Werder, D.; Stewart, M. H.; Klimov, V. I.; Hollingsworth, J. A. *J. Am. Chem. Soc.* **2004**, *126*, 11752−11753.
(6) Bakueva, L.; Gorelikov, I.; Musikhin, S.; Zhao, X. S.; Sargent, E. H.; Kumacheva, E. *Adv. Mater.* **2004**, *16*, 926−929.
(7) Harman, T. C.; Taylor, P. J.; Walsh, M. P.; LaForge, B. E. *Science* **2002**, *297*, 2229−2232.
(8) Murray, C. B.; Sun, S.; Gaschler, W.; Doyle, H.; Betley, T. A.; Kagan, C. R. *IBM J. Res. Dev.* **2001**, *45*, 47−55.
(9) Lee, S.-M.; Jun, Y.-w.; Cho, S.-N.; Cheon, J. *J. Am. Chem. Soc.* **2002**, *124*, 11244−11245.
(10) Lee, S.-M.; Cho, S.-N.; Cheon, J. *Adv. Mater.* **2003**, *15*, 441−444.
(11) Lu, W.; Fang, J.; Stokes, K. L.; Lin, J. *J. Am. Chem. Soc.* **2004**, *126*, 11798−11799.
(12) Lu, W.; Gao, P.; Jian, W. B.; Wang, Z. L.; Fang, J. *J. Am. Chem. Soc.* **2004**, *126*, 14816−14821.
(13) LaMer, V. K.; Dinegar, R. H. *J. Am. Chem. Soc.* **1950**, *72*, 4847−4854.
(14) Smet, Y. D.; Deriemaeker, L.; Finsy, R. *Langmuir* **1997**, *13*, 6884−6888.
(15) Grätz, H. *Scr. Mater.* **1997**, *37*, 9−16.
(16) Murray, C. B.; Kagan, C. R.; Bawendi, M. G. *Annu. Rev. Mater. Sci.* **2000**, *30*, 545−610.
(17) Wang, Z. L.; Petroski, J. M.; Green, T. C.; El-Sayed, M. A. *J. Phys. Chem. B* **1998**, *102*, 6145−6151.
(18) Petroski, J. M.; Wang, Z. L.; Green, T. C.; El-Sayed, M. A. *J. Phys. Chem. B* **1998**, *102*, 3316−3320.
(19) Wang, Z. L. *J. Phys. Chem. B* **2000**, *104*, 1153−1175.
(20) Qian, C.; Kim, F.; Ma, L.; Tsui, F.; Yang, P.; Liu, J. *J. Am. Chem. Soc.* **2004**, *126*, 1195−1198.
(21) Gabrisch, H.; Kjeldgaard, L.; Johnson, E.; Dahmen, U. *Acta Mater.* **2001**, *49*, 4259−4269.
(22) Zeng, H.; Rice, P. M.; Wang, S. X.; Sun, S. *J. Am. Chem. Soc.* **2004**, *126*, 11458−11459.